



Minerva Access is the Institutional Repository of The University of Melbourne

Author/s:

Khuong-Quang, DA;Brown, LM;Wong, M;Mayoh, C;Sexton-Oates, A;Kumar, A;Pinese, M;Nagabushan, S;Lau, L;Ludlow, LE;Gifford, AJ;Rodriguez, M;Desai, J;Fox, SB;Haber, M;Ziegler, DS;Hansford, JR;Marshall, GM;Cowley, MJ;Ekert, PG

Title:

Recurrent SPECC1L–NTRK fusions in pediatric sarcoma and brain tumors

Date:

2020-12-01

Citation:

Khuong-Quang, D. A., Brown, L. M., Wong, M., Mayoh, C., Sexton-Oates, A., Kumar, A., Pinese, M., Nagabushan, S., Lau, L., Ludlow, L. E., Gifford, A. J., Rodriguez, M., Desai, J., Fox, S. B., Haber, M., Ziegler, D. S., Hansford, J. R., Marshall, G. M., Cowley, M. J. & Ekert, P. G. (2020). Recurrent SPECC1L–NTRK fusions in pediatric sarcoma and brain tumors. *Cold Spring Harbor Molecular Case Studies*, 6 (6), <https://doi.org/10.1101/MCS.A005710>.

Persistent Link:

<https://hdl.handle.net/11343/252255>

License:

CC BY-NC

## TITLE PAGE

Recurrent *SPECCIL-NTRK* fusions in paediatric sarcoma and brain tumours

Dong-Anh Khuong-Quang<sup>1,2,3</sup>, Lauren M. Brown<sup>1,3,4</sup>, Marie Wong<sup>1,10</sup>, Chelsea Mayoh<sup>1</sup>, Alexandra Sexton-Oates<sup>3</sup>, Amit Kumar<sup>1,5</sup>, Mark Pinese<sup>1</sup>, Sumanth Nagabushan<sup>6</sup>, Loretta Lau<sup>1,6</sup>, Louise E. Ludlow<sup>3</sup>, Andrew J. Gifford<sup>1,7</sup>, Michael Rodriguez<sup>7</sup>, Jayesh Desai<sup>5,8</sup>, Stephen B. Fox<sup>8,9</sup>, Michelle Haber<sup>1</sup>, David S. Ziegler<sup>1,6</sup>, Jordan R. Hansford<sup>2,3,4</sup>, Glenn M. Marshall<sup>1,6</sup>, Mark J. Cowley<sup>1,10</sup> and Paul G. Ekert<sup>1,3,5,10</sup>.

1. Children's Cancer Institute, University of New South Wales, Randwick, 2031, Australia
2. Children's Cancer Centre, Royal Children's Hospital, Parkville, 3052, Australia
3. Murdoch Children's Research Institute, Royal Children's Hospital, Parkville, 3052, Australia
4. Department of Paediatrics, University of Melbourne, Parkville, 3052, Australia
5. Peter MacCallum Cancer Centre, Melbourne, 3000, Australia
6. Kids Cancer Centre, Sydney Children's Hospital, Randwick, 2031, Australia
7. Department of Anatomical Pathology, Prince of Wales Hospital, Randwick, 2031, Australia
8. Sir Peter MacCallum Department of Oncology, University of Melbourne, Australia
9. Department of Pathology, Peter MacCallum Cancer Centre, Melbourne, Australia
10. School of Women's and Children's Health, UNSW Medicine, UNSW Sydney, Randwick, 2031, Australia

Corresponding author: Associate Professor Paul G. Ekert, Group Leader, Translational Tumour Biology, Children's Cancer Institute, Randwick, NSW, Australia

Email: [PEkert@ccia.org.au](mailto:PEkert@ccia.org.au)

Short running title: Recurrent *SPECCIL-NTRK* fusions

Target journal: Molecular Case Studies

Article type: Research Article

ABSTRACT (160 words)

The identification of rearrangements driving expression of Neurotrophic Receptor Tyrosine Kinase (*NTRK*) family kinases in tumours has become critically important due to the availability of effective, specific inhibitor drugs. Whole genome sequencing (WGS) combined with RNA Sequencing (RNAseq) can identify novel and recurrent expressed fusions. Here we describe three *SPECCIL-NTRK* fusions identified in two paediatric central nervous system cancers and an extracranial solid tumour using WGS and RNAseq. These fusions arose either through a simple balanced rearrangement, or in the context of a complex chromoplexy event. We cloned the *SPECCIL-NTRK2* fusion directly from a patient sample and showed that enforced expression of this fusion is sufficient to promote cytokine-independent survival and proliferation. Cells transformed by *SPECCIL-NTRK2* expression are sensitive to a TRK inhibitor drug. We report here that *SPECCIL-NTRK* fusions can arise in a range of paediatric cancers. Whilst WGS and RNAseq are not required to detect *NTRK* fusions, these techniques may be of benefit when *NTRK* fusions are not suspected on clinical grounds or not identified by other methods.

## INTRODUCTION

Genomic and transcriptomic sequencing of paediatric cancers has broadened the spectrum of driver genetic alterations recognised across diverse tumour types. A subset of these drivers are targetable with novel therapies, which in some cases provides clinical options where none previously existed. The TRK family of receptors, encoded by the *NTRK1*, *NTRK2* and *NTRK3* genes, are proto-oncogenes regulating signalling pathways, including the MAPK and PI3K pathways, and play a critical role in neuronal development and differentiation. Fusions that link protein-protein interaction domains to the tyrosine kinase domain of each of the *NTRK* genes are recognised oncogenic drivers. *NTRK* fusions were first described in colorectal carcinoma (Martin-Zanca, D., *et al.*, 1986) and papillary thyroid carcinoma (Bongarzone, I., *et al.*, 1989), and later in a broad range of cancer types including paediatric cancers (Knezevich, S. R., *et al.*, 1998; Davis, J. L., *et al.*, 2018). *NTRK* fusions are strongly associated with particular rare paediatric tumour types, notably infantile fibrosarcoma (Knezevich, S. R., *et al.*, 1998), where 70-90% of cases harbor recurrent *ETV6-NTRK3* fusions (Bourgeois, J. M., *et al.*, 2000; Sheng, W. Q., *et al.*, 2001). *NTRK* fusions also characterise a subset of more common tumours, such as paediatric gliomas (Mackay, A., *et al.*, 2017; Clarke, M., *et al.*, 2020; Guerreiro Stucklin, A. S., *et al.*, 2019).

The clinical identification of *NTRK* fusions is a high priority due to the availability and clinical efficacy of TRK inhibitors (Drilon, A., *et al.*, 2018). The dramatic anti-tumoral activity of TRK inhibitors appears to be independent of the clinical features of the tumour in which it arises, including histological type, patient age, and genomic mechanisms generating the fusion (Drilon, A., *et al.*, 2018; Laetsch, T. W., *et al.*, 2018). Larotrectinib is only the second agent to be granted FDA-approval based on the presence of a molecular alteration, regardless of the type of cancer in which the mutation occurs, and a trial in previously untreated paediatric solid tumours is underway (COG ADVL1823 – NCT03834961). To emphasize the importance of detecting a potential *NTRK* fusion, the European Society for Medical Oncology (ESMO) Translational Research and Precision Medicine Working Group has recommended testing for *NTRK* fusions in all advanced stage malignancies, particularly if standard testing has not identified clear driver mutations (Marchio, C., *et al.*, 2019).

Whole genome sequencing (WGS) and whole transcriptome RNA sequencing (RNAseq) offer an unbiased methodology to identify the presence of all expressed structural variants such as *NTRK* fusions. *NTRK* fusions, either recurrent, rare or with unknown fusion partners

can also be detected with a range of next generation sequencing (NGS) approaches, including panels sequencing RNA after library preparation based on hybridisation capture or anchored multiplex PCR (Seager, M., *et al.*, 2019). More specific and sensitive genetic techniques including fluorescence in situ hybridisation (FISH) and PCR-based assays are efficient and rapid but are limited to known fusions and risk missing unique or rare recurrent *NTRK* fusions. Immunohistochemical techniques detect TRK overexpression as a surrogate for the presence of a driver fusion, but have limitations in specificity, particularly for *NTRK3* fusions (Penault-Llorca, F., *et al.*, 2019).

Here, we report the genomic features of three instances of a recurrent *NTRK* fusion partner, *SPECCIL*, in diverse paediatric cancer subtypes. The mechanisms giving rise to these fusions vary from simple reciprocal translocations to very complex chromosomal events resembling chromoplexy. We have cloned and expressed the *SPECCIL-NTRK2* fusion and show that it is sufficient to permit cytokine-independent survival and proliferation. These data emphasize the significant potential clinical benefit of performing WGS and RNAseq to identify recurrent targetable lesions in difficult-to-treat tumours in which driver lesions have not been identified by conventional testing.

## RESULTS

### Clinical presentation

Table 1 summarizes the clinical details of each of the three patients. Patient 1 presented with neurological symptoms of ataxia and intermittent headaches and was diagnosed at the age of 10 years with an unusual pineal low grade neuroepithelial tumour. The tumour has two morphologically distinct components. One contains a moderate density of mildly pleomorphic, strongly GFAP-positive, Olig2- and CD34-negative glial cells with extensive psammomatous calcification. The other component was more cellular, containing plump spindle-shaped and large epithelioid cells with occasional perivascular pseudorosettes resembling astroblastomatous pseudorosette. Most of these cells were also strongly GFAP positive although some of the epithelioid cells did not stain. The epithelioid cells were strongly CD34 immunoreactive. Both components were S100- and CD56-positive and did not stain for neurofilament protein, synaptophysin, chromogranin, IDH1 R132H, H3K27M or BRAFV600E. No mitotic figures were identified and the Ki67 labelling index was low (2-3%). No necrosis or microvascular proliferation were identified. The tumour could not be classified using the current (2016) WHO classification and consequently cannot be given a WHO grade although there were no high-grade features. The tumour was partially resected and third ventriculostomy performed. As part of an ongoing research project, DNA methylation profiling using the Illumina Infinium HumanMethylation 850k BeadChip and DNA panel sequencing as previously described (Sahm, F., *et al.*, 2016) were performed. Although the tumour did not match with any reference class of central nervous system tumour (highest score for the methylation class family low grade glioma, subclass ganglioglioma with a score of 0.71) using the DNA methylation-based classifier developed by the German Cancer Research Centre (DKFZ) (Capper, D., *et al.*, 2018), the DNA panel sequencing suggested the possibility of an *NTRK* fusion. *NTRK* fusions are not currently tested for as a part of standard of care clinical diagnostics for this type for tumour in Australia. However, research-based WGS and RNAseq identified a *SPECC1L-NTRK2* fusion. Currently the patient is not receiving any treatment and has stable residual disease without any sign of progression, 20 months after the surgery.

Patient 2 presented with seizures and focal neurological deficit and was diagnosed at the age of 16 months with an unresectable thalamic anaplastic astrocytoma (WHO grade III). The tumour presented dense and uniform cells with marked atypia, mitotic figures. No necrosis or microvascular proliferation was seen. The Ki-67 was approximately 10%, and the positive staining for WT-1, S100, and restricted GFAP expression as well as negative synaptophysin

staining are mostly in keeping with anaplastic astrocytoma. This tumour was negative for H3.3, H3.3B and H3.1 K27 and G34 mutations. No *BRAF* fusions or *BRAF* mutations were identified. The tumour progressed despite treatment with carboplatin-based chemotherapy as previously reported (Fouladi, M., *et al.*, 2009). RNAseq, performed as an adjunct to a clinical trial of targeted amplicon DNA sequencing (iPredict flagship, Melbourne Genomics Health Alliance (MGHA)), identified the *SPECCIL-NTRK2* fusion, which was confirmed by subsequent WGS. The patient was commenced on larotrectinib following enrolment onto a phase 1 clinical trial (NCT02637687), with no further disease progression and continues on therapy with stable disease for 33 months.

Patient 3 was diagnosed at the age of 11 months with a large congenital infantile fibrosarcoma of the chest wall compressing the lungs and airways. The tumour has a varied appearance. In areas (demonstrated in Figure 2), the tumour consists of intersecting fascicles of densely packed spindle cells with scant eosinophilic to amphophilic cytoplasm. Elsewhere the tumour contains fibrocollagenous stroma infiltrated with tumour cells which have more eosinophilic to vacuolated cytoplasm. The patient had no response to conventional chemotherapy and required intubation and ventilation with increasingly difficult ventilatory requirements. The presence of an *NTRK* fusion was suspected based on the histological diagnosis. *ETV6* break-apart FISH was performed on a biopsy specimen to identify an *ETV6-NTRK3* fusion and the result was negative. A *SPECCIL-NTRK3* fusion was identified by WGS and RNAseq. The patient was commenced on larotrectinib with excellent clinical response and near complete resolution of disease on radiological imaging.

### Genomic Analyses

The variant table (Table 2) shows the details of the *SPECCIL-NTRK* fusions, including the genomic breakpoints and the sequencing platforms used to identify the fusions. The range of somatic single nucleotide variants (SNV), copy number variants (CNV), and structural variants (SV) are shown in Supplementary Table 1. All three samples were sequenced as part of studies in which somatic and germline sequencing is performed to identify potential clinically actionable variants (Wong, Marie, *et al.*, 2020). In each patient, the *NTRK* fusion was identified as the highest priority actionable target. The SNV tumour mutation burden was < 1 mutation/Mb in each instance.

The somatic genomes of the *SPECCIL-NTRK* fusions are summarised in the Circos plots shown in Supplementary Figure 1. In all three patients, the *NTRK* fusions are also annotated as potentially linked to the *ADORA2A* gene (ENST00000337539), which is located at the

same locus as *SPECCIL* and a *SPECCIL-ADORA2A* read through transcript is included in the reference genome. However, the expressed fusions include only *SPECCIL* (Figure 1A-E). The tumour from Patient 1 harboured multiple whole chromosomal gains in contrast to the tumour from Patient 2, which was less aneuploid but harboured a bi-allelic loss of *CDKN2A/B* (chr9). The *SPECCIL* breakpoints in Patients 1 and 2 also differed, in intron 12 and intron 11 respectively (Figure 1A and B and Table 2), however, in each instance the fusion remained in frame. The *SPECCIL-NTRK3* fusion (Patient 3) arose from a complex chromoplexy event involving multiple structural variants and copy number aberrations on chromosome 15 (Supplementary Figure 1D). An inversion involving exons 14 to 19 of *NTRK3*, encoding the tyrosine kinase domain, resulted in an in-frame fusion to the first nine exons of *SPECCIL* (Figure 1C-E). In each case, although the *SPECCIL* breakpoint differs, the SMC (Structural Maintenance of Chromosomes) domain of *SPECCIL*, which is involved in heterodimerization of SMC protein family members and contains an extended coiled-coil region, is retained in frame with the tyrosine kinase domains of *NTRK2* or *NTRK3*. Immunohistochemistry confirmed the expression of TRK in all three tumours (Figure 2). Linx, which clusters together contemporaneous individual copy number changes and structural variant calls, was used to provide a visualization of the structure of derivative chromosomes (Cameron, Daniel L., *et al.*, 2019) (Figure 3). Patient 1 had a duplication encompassing *NTRK2* tyrosine kinase domain linked to *SPECCIL* SMC domain (copy number = 2). The derivative chr22 included small regions with varying copy number states, but which did not involve *SPECCIL* or *NTRK2* (Figure 3B). The fusion in Patient 2 is a simple reciprocal translocation (Figure 3C). The *SPECCIL-NTRK3* fusion has arisen from a much more complex event, with a derivative chromosome including break ends in chr15, chr22 and chrX (Figure 3D). The predicted fusion is flanked by more than 70 breakpoints associated with several copy number states, a pattern consistent with chromoplexy (reviewed in (Shen, M. M., 2013)). The very complex structural variants in chr15 of patient 3 were the primary genomic feature of this tumour. The expressed *NTRK3* fusion is the likely mechanism favouring selection of this chromoplexy event in this tumour. We additionally performed targeted sequencing (TSO500 panel – Tru-Sight Oncology 500 gene panel, Illumina) on formalin-fixed paraffin embedded tissue from a resected sample from Patient 3 after 22 months of larotrectinib therapy. No known resistance mutations in *NTRK3* were found (Cocco, E., *et al.*, 2018) but evidence of reads spanning the original fusion breakpoint were identified, confirming persistent expression of the *SPECCIL-NTRK3* fusion in residual tumour tissue (Supplementary Figure 2).

## Functional Analyses

We cloned the *SPECC1L-NTRK2* fusion directly from cDNA derived from tumour RNA from the Patient 2 sample. There were two potential start sites that permitted transcription of an in-frame construct. The first was a full-length (FL *SPECC1L-NTRK2*) version of the fusion (transcription from the canonical start site of *SPECC1L*). The second was a truncated form (T *SPECC1L-NTRK2*) predicted to start from *SPECC1L* amino acid coding position 667 (ENST00000314228.9). The full-length form was the dominant transcript and we could not exclude the possibility that the truncated form was a PCR artefact. Both transcripts were expressed in interleukin-3 (IL-3) dependent Ba/F3 cells under the regulation of a doxycycline-inducible promoter (Figure 4A). Upon doxycycline addition, FL and T *SPECC1L-NTRK2* fusion proteins were detected at their predicted sizes, 142kDa and 69kDa, respectively, using a pan-Trk antibody (Figure 4A). When IL-3 was removed from cultures, we observed increased expression of both fusions, likely the result of selection in favour of cells expressing higher levels of the fusion, and apoptosis of cells not expressing, or expressing low levels of the fusion.

We then cultured the fusion-expressing cells and empty vector controls in the presence or absence of IL-3 over a 10 day time course (Figure 4B), to assess the capacity of *SPECC1L-NTRK2* to promote long-term IL-3 independent proliferation in Ba/F3 cells. The number of FL and T *SPECC1L-NTRK2*-expressing viable cells increased over time in the absence of IL-3. In contrast, empty vector (pFTRE) control cells were dead by day 10 of IL-3 withdrawal (Figure 4B). These data show that both the full length and truncated *SPECC1L-NTRK2* fusion blocks IL-3 withdrawal-induced apoptosis and drives IL-3 independent proliferation in Ba/F3 cells.

Following the generation of stably transformed Ba/F3 cell lines with *SPECC1L-NTRK2* fusions, we next assessed the sensitivity of fusion expressing cells to a TRK inhibitor, larotrectinib. Control cells (maintained in IL-3) remained viable at all doses of larotrectinib and imatinib (tyrosine kinase inhibitor specific against ABL1, c-KIT and PDGFR). FL *SPECC1L-NTRK2* and T *SPECC1L-NTRK2* expressing Ba/F3 cells, in which fusion expression is required to maintain viability in the absence of IL-3, died when exposed to a 7-point dose titration of larotrectinib but not imatinib (Figure 4C). These data demonstrate that Ba/F3 cells transformed by FL *SPECC1L-NTRK2* and T *SPECC1L-NTRK2* fusions are specifically sensitive to TRK inhibitor treatment.



## DISCUSSION

We report here three examples of recurrent *NTRK* fusions identified in three paediatric patients with three different histological diagnoses. This fusion is not detectable by routine FISH and highlights the role of genome-wide approaches like WGS and RNAseq, in identifying diagnostic and therapeutic targets. The *SPECCIL-NTRK2* fusion has been reported recently in paediatric glioma with anaplastic features (Torre, Matthew, *et al.*, 2020), and in paediatric mixed neuronal glial tumour (Surrey, L. F., *et al.*, 2019) while the *SPECCIL-NTRK3* fusion has been seen in undifferentiated sarcomas of the uterus (Rabban, J. T., *et al.*, 2020; Gatalica, Z., *et al.*, 2019; Hodgson, A., *et al.*, 2020) and in mesenchymal tumours of the gastrointestinal tract (Atiq, M. A., *et al.*, 2020). *SPECCIL* is a gene encoding a coiled-coil domain protein located on 22q11.23. Germline loss-of-function mutations in *SPECCIL* have been identified in patients with oblique facial clefts (Saadi, I., *et al.*, 2011). Several recurrent partner genes have been reported to fuse with *SPECCIL*, including *RET*, which leads to constitutive RET kinase activation in papillary thyroid carcinomas (Cancer Genome Atlas Research, Network, 2014; Stransky, N., *et al.*, 2014), *MET* in lung adenocarcinoma (Nelson, A. W., *et al.*, 2019), and *ALK* in epithelioid fibrous histiocytoma (Dickson, B. C., *et al.*, 2018).

The *SPECCIL* SMC coiled-coil domains are retained in each of the *NTRK* fusion genes. Coiled-coil domains have been shown to play a role in activation of receptor tyrosine kinases by promoting dimerization and transphosphorylation. This was first shown for MET receptor (Rodrigues, G. A., *et al.*, 1993) and the BCR-ABL fusion protein (McWhirter, J. R., *et al.*, 1993), but evidence has since been extended to other oncoproteins including TRK fusions (Cocco, E., *et al.*, 2018). For many *NTRK* fusions, the fusion partner mediates activation of the receptor via dimerization, either through the addition of one of three known dimerization domains: coiled-coil, zinc finger or WD domains, to the kinase domain of TRK or through alternate mechanisms (Cocco, E., *et al.*, 2018). We confirmed the oncogenic properties of the *SPECCIL-NTRK2* fusion *in vitro*, where transformed Ba/F3 cells gained the capacity to grow independently of IL-3 and were specifically sensitive to larotrectinib. However, while Ba/F3 is a gold-standard cell line model for exploring kinase-activating oncogenes *in vitro* (Roberts, K. G., *et al.*, 2014), and is a suitable model for first-pass assessment of the transforming capacity of this fusion, future work exploring the molecular mechanisms of oncogenesis by *SPECCIL-NTRK2* will require the modelling of this fusion in the same cellular context in which *SPECCIL-NTRK2* positive tumours arise.

In addition to the canonical *ETV6-NTRK3* fusion, novel *NTRK* fusions have been identified in an increasing number of tumour types, both in children and adults. This includes paediatric soft-tissue sarcomas (Pavlick, D., *et al.*, 2017; Davis, J. L., *et al.*, 2018) and gliomas as reported here and elsewhere (Mackay, A., *et al.*, 2017; Guerreiro Stucklin, A. S., *et al.*, 2019; Clarke, M., *et al.*, 2020). Given the clinical implications for patients, it is now critical to identify these fusions at diagnosis as TRK inhibitors are increasingly being integrated into patient treatments.

Whilst pan-TRK immunohistochemistry, which detects TRK overexpression as a surrogate for the presence of *NTRK* fusion, is a highly sensitive tool to identify *NTRK* fusions at low cost and with a fast turnaround time, there are caveats that apply to this technique (Marchio, C., *et al.*, 2019). Most notably, the specificity is limited in tissues with physiological TRK protein expression, such as in the nervous system and smooth muscle (Murphy, D. A., *et al.*, 2017). For example, diffuse immunoreactivity is observed in 8% of spindle cell tumours without *NTRK* fusions (Hung, Y. P., *et al.*, 2018). Moreover, the presence of an *NTRK* fusion may be associated with relatively weak pan-TRK staining (reviewed in (Marchio, C., *et al.*, 2019)). Pan-TRK IHC also has limited specificity particularly for *NTRK3* fusions (Penault-Llorca, F., *et al.*, 2019). Therefore, confirmation of the fusion by a second assay is widely recommended (Murphy, D. A., *et al.*, 2017; Marchio, C., *et al.*, 2019). The tumour resected after 22 months of treatment with larotrectinib from Patient 3 did not stain at all with pan-TRK antibody (data not shown), despite the presence of the fusion in residual tumour. One explanation is that the acid decalcification step used prior to fixation and staining abolishes antibody detection of the epitope in fixed material.

Break-apart FISH is a cost-effective and well-recognised method to detect recurrent gene fusions. Due to the high prevalence of *ETV6-NTRK* fusions, an *ETV6* probe has typically been used, despite a high false negative rate of up to 36% (Davis, J. L., *et al.*, 2018). It also fails to identify the *NTRK* partner gene. Therefore, *NTRK* break-apart FISH has been developed with a separate probe required for each of the three *NTRK* genes, making the test increasingly labour-intensive. Such tests are mostly recommended in the context of a tumour type with frequent *NTRK* fusion (Marchio, C., *et al.*, 2019), and do not exclude further testing if the result is negative. In the case of Patient 3, the *ETV6* break-apart FISH testing failed to identify the *NTRK* fusion.

NGS is the method with the highest specificity and sensitivity to detect gene fusions compared to other testing methods, however access may be limited due to the availability of the technique and its associated cost. Although DNA-based NGS panels are widely used in

cancer, the detection of the fusion will depend on the platform used given that *NTRK2* and *NTRK3* genes have large introns that are typically inadequately sequenced, and therefore difficult to analyse. To illustrate this difficulty, the *NTRK2* fusion reported in Patient 2 was not detected by the custom targeted amplicon DNA sequencing performed as neither the *NTRK2* intron or the *SPECCIL* exons and introns involved in the fusion were included in the gene panel design. However, the fusion was detected by targeted panel sequencing in relapse material from Patient 3. RNA-based NGS panel based on hybridisation capture or anchored multiplex RT-PCR allows for detection of unknown partners and both methods are currently used in the clinical setting (Hsiao, Susan J., *et al.*, 2019; Jennings, L. J., *et al.*, 2017). In conclusion, we report three cases of recurrent *SPECCIL-NTRK* fusions in diverse paediatric malignancies. The fusions were definitively identified by high throughput sequencing approaches that combined WGS and RNAseq. WGS and RNAseq are a highly effective and unbiased combination to identify these and other fusions.

## METHODS

### Whole genome sequencing

For primary tumour tissue, DNA was extracted from fresh-frozen tissues using the AllPrep DNA/RNA/Protein Mini Kit (QIAGEN 8004) according to the manufacturer's instructions. Whole genome sequencing (WGS) to intended coverage depths of 30X (normal tissue) and 90X (tumour tissue) was performed using Illumina's HiSeq X platform. Library preparation was performed using the TruSeq Nano DNA HT or Kapa HyperPrep PCR-free kit following the manufacturer's instructions. Details of sequencing coverage are presented in Supplementary Table 2.

WGS data was processed using the in house *refynr* pipeline, utilising DNAnexus ([www.dnanexus.com](http://www.dnanexus.com)), a cloud-based genomic analysis platform. Paired-end short reads were aligned to the hs37d5 reference genome, using BWA-MEM (v017.10-r789; (Li, H., *et al.*, 2009)) and duplicate reads marked and data from multiple lanes merged using Novosort (v1.03.01; default settings), followed by GATK IndelRealigner (v3.3; (Van der Auwera, G. A., *et al.*, 2013)). Germline SNVs and short indels (<50-bp) were identified using GATK HaplotypeCaller, GenotypeVCFs and VQSR (v3.3; (Van der Auwera, G. A., *et al.*, 2013)), annotated with VEP (v87; (McLaren, William, *et al.*, 2016)), converted into a database using GEMINI (v0.11.0; (Paila, U., *et al.*, 2013)), and imported into Seave (Gayevskiy, V., *et al.*, 2019) for filtration and prioritization. Somatic SNVs and short indels (<50-bp) were identified using Strelka (v2.0.17; (Saunders, C. T., *et al.*, 2012)) and filtered using these criteria:  $QSS \geq 10$  or  $QSI \geq 10$ ; NT=ref; from chromosomes 1-22,X,Y; in at most 3 (of 2,570) individuals in the similarly processed MGRB cohort (Pinese, Mark, *et al.*, 2020); if not in the platinum genome's high confidence region then with  $VAF > 0.1$  and  $QSS > 20$  or  $QSI > 20$ ;  $VAF * QS \geq 1.3$ ; Normal AF > 0 and Tumor AF < 3 \* normal AF; or in a curated hotspot white list. Somatic variants were annotated using SnpEff (v4\_3t; (Cingolani, P., *et al.*, 2012)) and imported into in house *Glooe* platform for filtration and prioritization. Tumour purity and somatic CNV were assessed using PURPLE (v2.39, (Cameron, Daniel L., *et al.*, 2019)). Somatic structural variants were identified using GRIDSS (v2.7.2) and derivative chromosomes analysed and visualised using Linx (v1.7; (Cameron, Daniel L., *et al.*, 2019)) using default settings.

### Whole transcriptome data analysis

Whole transcriptome RNA sequencing (RNAseq) was performed with TruSeq stranded mRNA preparation kit. Libraries were pooled and sequencing runs were performed in paired-

end mode using either the Illumina HiSeq 4000 platform or NextSeq generating approximately 40M reads per sample respectively. Illumina paired-end RNAseq data was aligned to the human genome assembly (build hg19) using STAR (version 2.5) 2-pass method with quantMode parameters set to TranscriptomeSAM for alignments translated into transcript coordinates. Alignments are sorted with SAMTools (version 1.3.1), duplicates marked with Picard Tools (version 2.4.1), reads are split and trimmed, and mapping qualities reassigned with Genome Analysis Toolkit (version 3.6) using methods SplitNCigarReads and ReassignOneMappingQuality respectively. Raw gene counts, TPM, FPKM and isoform expression values were calculated using RSEM (version 1.2.31) command rsem-calculate-expression. Fusions were identified using three methods, STAR-Fusion (version 1.3.1), JAFFA (version 1.09) and arriba (version 1.1.0). All fusions were reported as either High-, Medium-, or Low-Confidence, whether they were in-frame or not, and the type of rearrangement.

#### TSO500 DNA/RNA panel

##### Bioinformatic analysis of TSO500

DNA and RNA were extracted from FFPE blocks using standard protocols at the KCCG Cancer Diagnostics laboratory. DNA paired-end reads were processed using the Illumina TruSight Oncology 500 Local App (v1.0) Docker container, run on the DNAnexus platform using default options. RNA paired-end reads (14M reads) were aligned to hg19 using STAR (v2.5) 2-pass method, duplicates marked with Picard Tools (v2.4.1), reads split and trimmed and mapping qualities reassigned with GATK (v3.6) using methods SplitNCigarReads and ReassignOneMappingQuality respectively. Variants were identified using GATK HaplotypeCaller and *NTRK3* variants were inspected for previously reported resistance mutations. *NTRK3* SNPs were observed at a maximum read depth of approximately 450 reads. Fusions were identified using arriba (v1.1.0).

#### TRK Immunohistochemistry

Immunohistochemistry staining for TRK A, B and C expression was performed on paraffin-embedded sections using the BenchMark ULTRA system (Roche, Castle Hill, Australia) using the pan-TRK monoclonal antibody clone EPR17341 (Roche/Ventana, Castle Hill, Australia).

### *SPECC1L-NTRK2* fusion cloning

Patient RNA was reverse transcribed into cDNA using the SuperScript III First-Strand Synthesis System (Thermo Fisher Scientific). Truncated *SPECC1L-NTRK2* (T *SPECC1L-NTRK2*) was amplified from patient cDNA using *SPECC1L* Exon4 kozac F forward primer and *NTRK R* reverse primer (see Table 3). Full length *SPECC1L-NTRK2* (FL *SPECC1L-NTRK2*) was amplified from patient cDNA using *SPECC1L* FL F forward primer and *NTRK R* reverse primer (Supplementary Table 2). Fusions were PCR amplified using GoTaq® Long PCR Master Mix (Promega) as per manufacturer's instructions. Truncated and full length *SPECC1L-NTRK2* fusions were cloned into the pFTRE tight mTAad GFP (pFTRE GFP) lentiviral vector using the EcoRI restriction site. Fusion sequences were confirmed by Sanger sequencing (Australian Genome Research Facility).

### Cell culture and retroviral transduction and infection

For lentiviral transduction, HEK293T cells were transfected using Effectene reagent (QIAGEN), using pCMV-dR8.2 dvpr packaging vector and pMD2.G VSV-G envelope. Ba/F3 cells were transduced with lentivirus encoding pFTRE GFP (control construct), T *SPECC1L-NTRK2*, and FL *SPECC1L-NTRK2* by spin infection and Polybrene reagent (Sigma Aldrich). GFP positive (fusion expressing) Ba/F3 cells were sorted by flow cytometry following transduction. Cell lines were maintained in RPMI 1640 medium (Sigma Aldrich) supplemented with 10% fetal bovine serum (FBS, Thermo Fisher Scientific) and 0.5 ng/mL recombinant murine IL-3 (Peprotech), at 37°C and 5% CO<sub>2</sub>. For induction, 1µg/mL of doxycycline was added to cultures, and fusion-expressing cells were maintained in RPMI supplemented with 10% FBS following selection.

### Western blotting

Western blot analysis was performed with antibodies targeting pan-TRK (EPR17341, Abcam, Cambridge, MA) and β-actin (Sigma Aldrich), as per manufacturer's instructions. HRP-conjugated secondary antibodies (GE healthcare) were used, and signal was detected using Luminata™ Forte Western HRP substrate (Millipore) and ChemiDoc™ XRS+ Imaging System (Bio-Rad Laboratories).

### Trypan blue cell count assay

Cell lines were washed three times in phosphate-buffered saline (PBS) to remove residual IL-3 from maintenance culture. Washed cells were then counted and seeded at 10<sup>5</sup> live cells/mL

in 24-well plates in RPMI supplemented with 10% FBS and 1 $\mu$ g/mL doxycycline, with and without IL-3 0.5ng/mL, and incubated at 37°C and 5% CO<sub>2</sub> for 10 days. Live cells were counted by trypan blue exclusion, using TC20™ Automated Cell Counter (Bio-Rad Laboratories) at 0, 3, 5, 7, and 10 days. Cells were maintained between 0.1-2 x 10<sup>6</sup>cells/mL and were diluted at each timepoint to prevent overgrowth. Data were analysed and visualised using GraphPad Prism v7.0 Software (GraphPad Software, Inc). Experiment was performed on two biologically independent lines in two independent technical replicates (n=4). All data is presented as Mean  $\pm$  standard error of the mean (SEM).

#### Drug treatment assay

Cell lines were washed in PBS, counted, and seeded at 10<sup>4</sup> live cells in 96-well plates in the presence (pFTRE empty vector control) or absence of 0.5 ng/mL IL-3, and 1 $\mu$ g/mL doxycycline. Cells were treated with 0.0024-10 $\mu$ M dose range of imatinib or larotrectinib (Selleck Chemicals), or vehicle control (dimethyl sulfoxide, DMSO, Sigma Aldrich). Drug treatment plates were incubated at 37°C and 5% CO<sub>2</sub> for 48 hours. Propidium iodide (PI) exclusion was measured using an LSR X-20 Fortessa and high-throughput sequencer (HTS) (BD Biosciences). Data were analysed using FlowJo™ v10.4 (FlowJo LLC) and GraphPad Prism v7.0 Software. Experiment was performed on two biologically independent lines in two independent technical replicates (n=4). All data is presented as Mean  $\pm$  standard error of the mean (SEM).

## ADDITIONAL INFORMATION

### Ethics statement

The study was approved by the Hunter New England Human Research Ethics Committee (Australia) with full written consent obtained from the parents, providing consent for the patients.

### Data depository and Access

The primary sequence data related to these cases is available through the European Genome-phenome Archive under the study ID [EGAS00001004679](https://www.ebi.ac.uk/ega/home) (<https://www.ebi.ac.uk/ega/home>).

### Acknowledgments

Tumour samples were supplied by the Children's Cancer Centre Tissue Bank at the Murdoch Children's Research Institute and The Royal Children's Hospital ([www.mcri.edu.au/childrenscancercentretissuebank](http://www.mcri.edu.au/childrenscancercentretissuebank)). Establishment and running of the Children's Cancer Centre Tissue Bank is made possible through generous support by Cancer In Kids @ RCH ([www.cika.org.au](http://www.cika.org.au)), the Royal Children's Hospital Foundation and the Murdoch Children's Research Institute.

### Author contributions

DAKQ and PGE conceived, designed and coordinated the study, L.M.B., A.S.O., D.A.K.Q., P.G.E. performed the *in vitro* experiments and analysed data. M.W., C.M., A.K., M.P., S.B.F., M.J.C., P.G.E. performed bioinformatics analysis, A.J.G. and M.R. reviewed the histology and performed the IHC, A.J.G., L.E.L. contributed materials, D.A.K.Q., S.N., L.L., D.S.Z., J.R.H., G.M.M. provided clinical data, J.D. and M.H. lead the precision medicine programs which provided the sequencing. D.A.K.Q., L.M.B. and P.G.E. wrote the original draft. All authors contributed to the written manuscript and approved the final manuscript.

### Funding

iPredict is a Flagship project of Melbourne Genomics and funded by the State Government of Victoria (Department of Health and Human Services) and the 10 member organisations of the Melbourne Genomics Health Alliance. S.J.F. acknowledges the support of the National Health and Medical Research Council (NHMRC) Grant Funding APP1079329. P.G.E. acknowledges the support of NHMRC Project Grant APP1140626, the Samuel Nissen Charitable Foundation and the Steven Walter Children's Cancer Foundation. G.M.M. acknowledges the support of Hyundai 4K and Steven Walter Children's Cancer Foundation. ZERO is a national study of precision medicine in paediatric cancer supported by the

Australian Federal Government Department of Health, New South Wales State Government, the Australian Cancer Research Foundation (ACRF), The Kids Cancer Alliance, Cancer Therapeutics Cooperative Research Centre (CTx CRC), Tour de Cure (tumour biobank personnel), Lions Kids Cancer Genome Project (WGS and personnel), Cure Brain Cancer Foundation, The Kids Cancer Project, University of New South Wales, Australian Genomics Health Alliance, Luminesce Alliance, The Medical Research Future Fund (MRFF) Australian Brain Cancer Mission, Minderoo Foundation's Eliminate Cancer Initiative, Zero Childhood Cancer Capacity Campaign, The Kinghorn Foundation, the Cancer Institute NSW and NSW Health (Fellowship funding for M.J.C.). Cancer Australia for personnel and computational support (APP1165556 to M.J.C.).

Zero Childhood Cancer is a joint initiative led by Children's Cancer Institute and Sydney Children's Hospital Randwick.

#### Competing Interest Statement

The authors have declared no competing interest.

## FIGURES AND TABLES

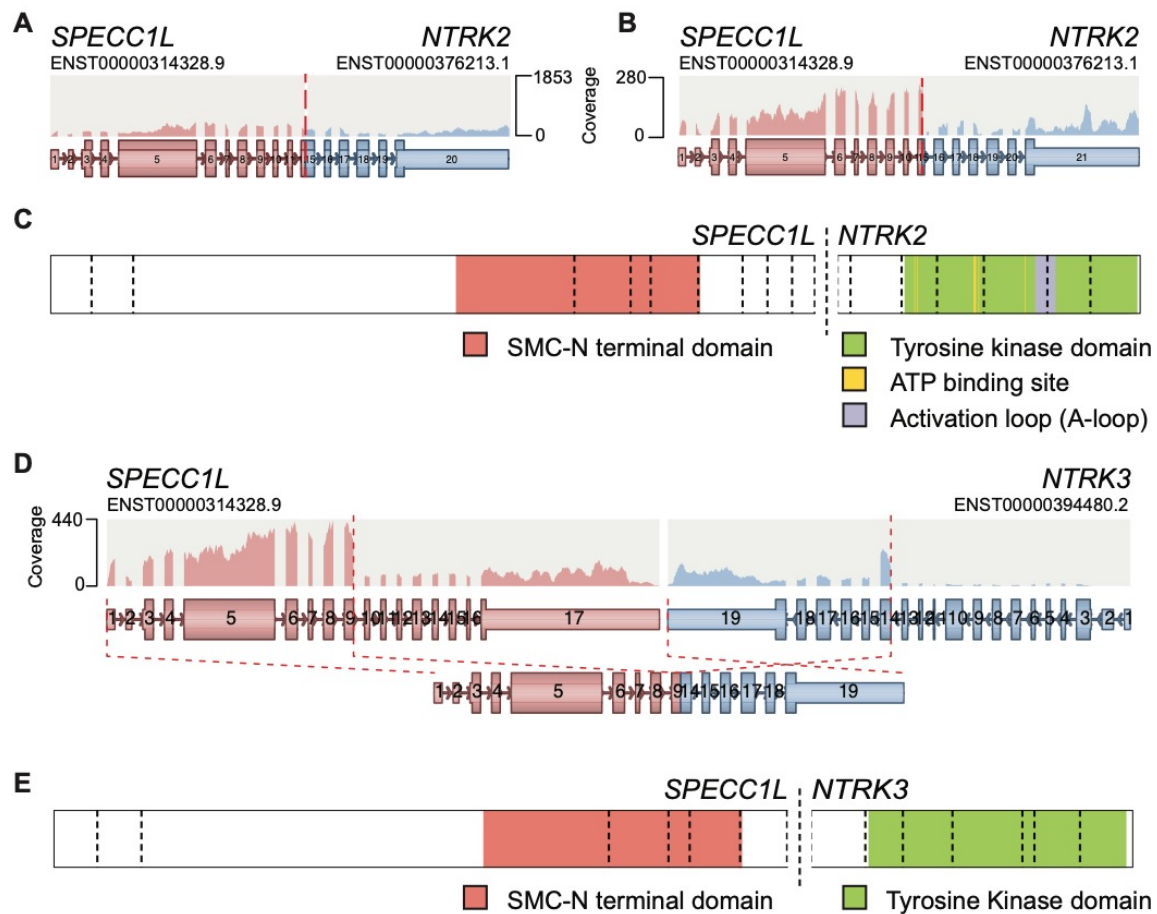


**Figure 1. *SPECC1L-NTRK* Fusions arising in an infantile fibrosarcoma and two paediatric central nervous system tumours**

A and B. *SPECC1L-NTRK2* fusions identified in patients 1 and 2 from transcriptomic data. RNAseq data was analysed using the Arriba algorithm (see Methods section), and the visualizations are modified from the Arriba output. The *SPECC1L* and *NTRK2* Ensembl reference transcripts are indicated above the read coverage in each gene. The breakpoints are indicated by the dashed red line. The structure of the in-frame fusion and the involved exons is shown.

C. Representation of the *SPECC1L-NTRK2* fusion generated using Protein Paint (Zhou, X., *et al.*, 2016), showing the conserved protein domains in the fusion protein. Key for protein domains retained in the fusion protein is shown below the schematic.

D. Arriba analysis of patient 3 and the *SPECC1L-NTRK3* fusion. Note the inversion of the exons encoding the tyrosine kinase domain of *NTRK3* that results in the in-frame fusion.

E. Representation of the *SPECC1L-NTRK3* fusion generated using Protein Paint, showing the conserved protein domains in the fusion protein.

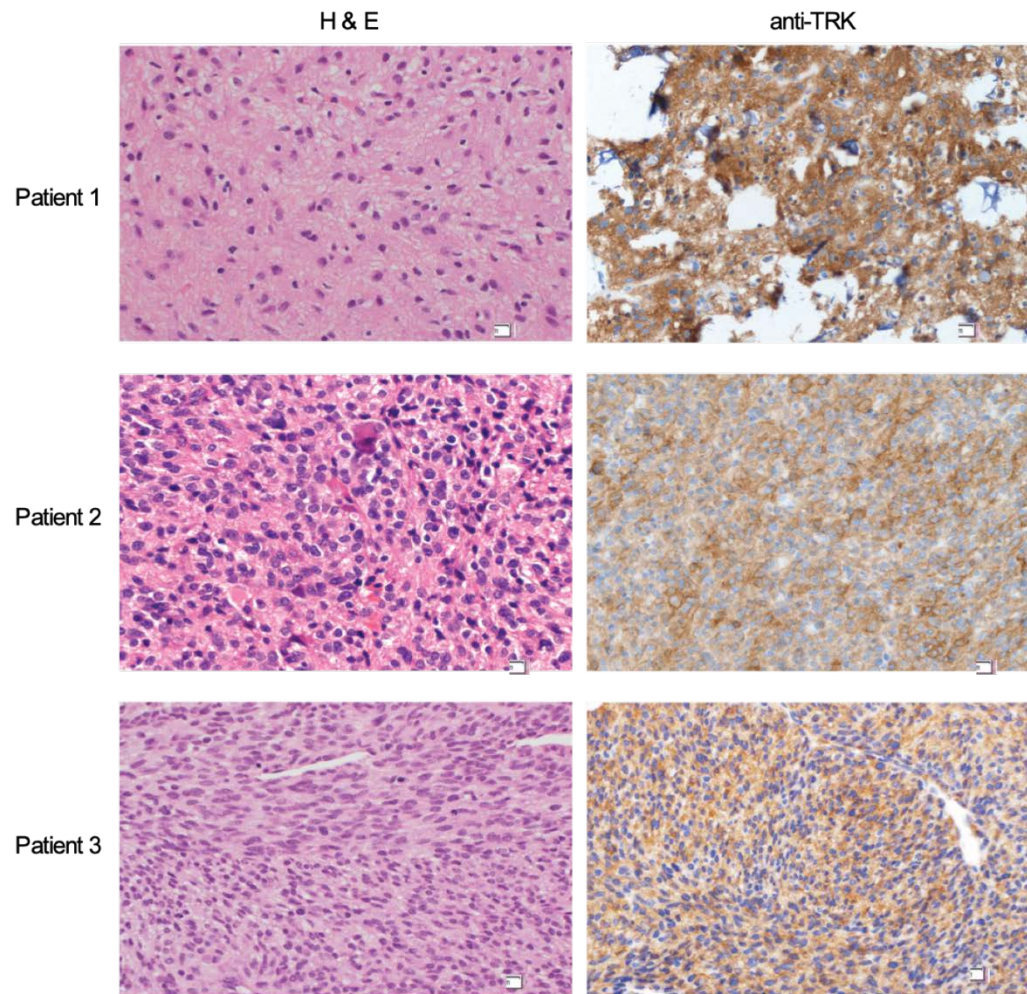


**Figure 2. Immunohistochemistry of *SPECCIL-NTRK* fusion positive tumours shows high TRK expression**

Hematoxylin and Eosin staining and anti-TRK staining are shown for each of the patient tumour samples. Non-neoplastic cells served as internal negative control for the TRK antibody and TRK expression was high for Patient 1, Patient 2 and Patient 3. Patient 1 presented with an unusual low grade neuroepithelial tumour, Patient 2 with an anaplastic astrocytoma and Patient 2 with an infantile fibrosarcoma. Further histologic description is detailed in the Clinical Presentation section in the main text.

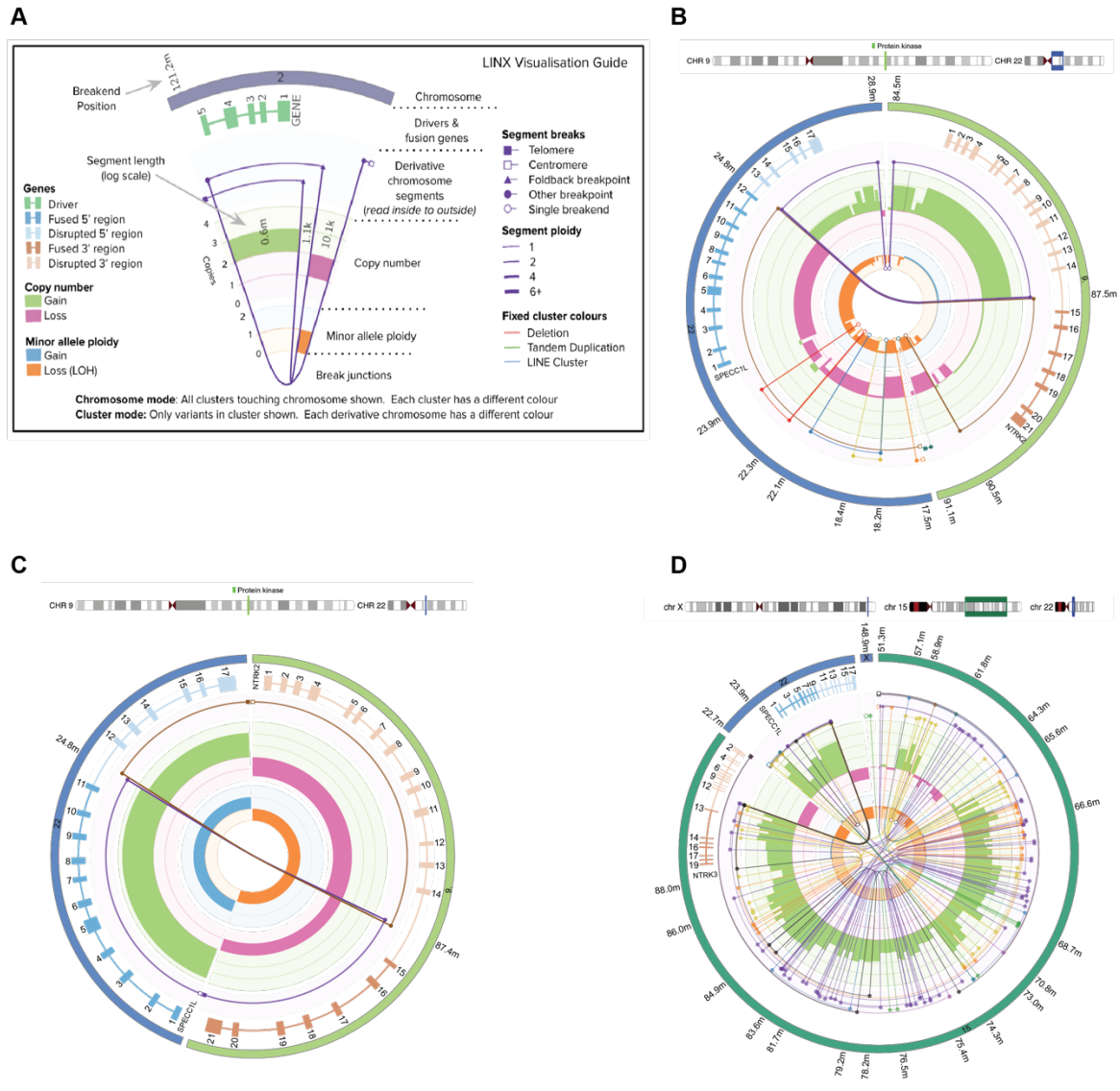


**Figure 3. Linx plots of the derivative chromosomes encoding each of the *NTRK* fusions**

A. Key for the interpretation of the Linx plots. This is reproduced with permission from (Cameron, Daniel L., *et al.*, 2019).

B. Linx plot of patient 1. This shows the fusion arising in association with a duplication event of *NTRK2* with linked break-ends juxtaposing the tyrosine kinase domain with *SPECCIL* SMC domain on chromosome 22. Other linked segments with variable copy number alterations in the chromosome 15 part of the derivative chromosome not associated with the fusion.

C. The *NTRK2* fusion in patient 2 is a simple reciprocal translocation associated with a copy number gain of *SPECCIL* and loss of one copy of the region encoding the tyrosine kinase domain of *NTRK2* (exons 15 – 21) and homozygous deletion of exon 1-14 of *NTRK2*. copy number loss (LOH) of *NTRK2*.

D. The *NTRK3* fusion arises from a complex structural event resembling chromoplexy, with multiple copy number states and more than 70 breakpoints in the derivative chromosome. The regions of the *NTRK3* and *SPECCIL* genes not involved in the fusion event are present as single copies only, having undergone a deletion event.

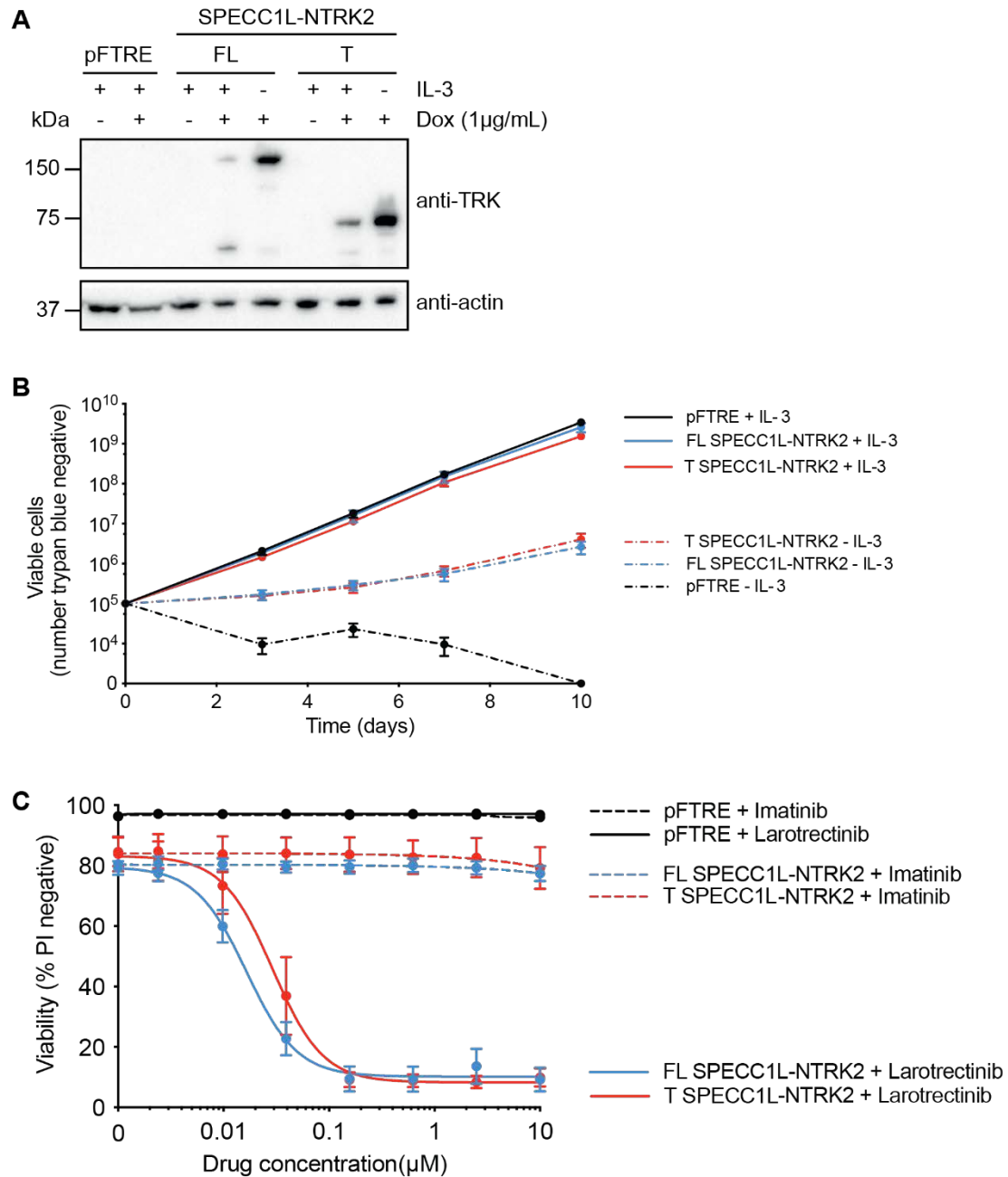


**Figure 4. *SPECC1L-NTRK2* fusions transform Ba/F3 cells to cytokine independence and these cells are sensitive to treatment with larotrectinib**

A. Western blot analysis of Ba/F3 cells expressing Full length (FL) and Truncated (T) *SPECC1L-NTRK2* fusions, and empty vector controls (pFTRE). Cells were maintained in the presence (+) or absence of IL-3 (-), and fusion expression was driven by the addition of doxycycline (Dox) to cultures. Western blot probed with anti-TRK and anti- $\beta$ -actin (anti-actin) was used as a loading control.

B. Viability analysis of doxycycline induced Ba/F3 cells seeded in the presence (solid line) and absence (dashed line) of IL-3. Number of viable cells, measured by trypan blue exclusion, is shown on the y-axis, and time in days from seeding in the presence or absence of IL-3 is shown on the x-axis (Data presented as Mean  $\pm$  SEM, n=4).

C. Viability analysis of *SPECCIL-NTRK2* transformed Ba/F3 cells following TKI treatment. Ba/F3 cells transformed with FL *SPECCIL-NTRK2* (blue line) or T *SPECCIL-NTRK2* (red line), and empty vector controls (pFTRE, black line) were treated with a dose titration of imatinib (dashed line) or larotrectinib (solid line) for 48 hours. Graph shows viability (%) on the y-axis, determined by flow cytometry and PI exclusion, and the x-axis depicts increasing drug concentration in  $\mu$ M. (Data presented as Mean  $\pm$  SEM, n=4).

**Table 1. Summary of patient characteristics**

<b>Gender</b>	M	M	F
<b>Age</b>	10 years	16 months	11 months
<b>Clinical presentation</b>	Three weeks history of dizziness, ataxia, and intermittent headaches	Epilepsy and focal neurological deficit	Failure to thrive, developmental regression, and intermittent fevers. Acute respiratory distress
<b>Diagnosis</b>	Low grade neuroepithelial tumour	Anaplastic astrocytoma	Infantile fibrosarcoma
<b>Primary tumour</b>	Pineal	Left thalamus	Chest
<b>Staging</b>	Localised	Localised	Localised
<b>Histopathology</b>	Low grade neuroepithelial tumour	Anaplastic astrocytoma	Congenital infantile sarcoma
<b>Ki67 staining</b>	Ki67 2-3%	Ki67 10%	Ki67 10%
<b>Pre-treatment</b>	Surgery alone	Carboplatin-based infant regimen (five cycles before tumour progression)	VCR/Cyclo/ActD followed by VCR
<b>Other reportable findings</b>	-	Homozygous loss of <i>CDKN2A/B</i>	-
<b>Treatment</b>	Surveillance	Larotrectinib	Larotrectinib
<b>Status</b>	SD 22 months post-surgery	SD on larotrectinib for 33 months	CR post-surgery after 22 months on larotrectinib

Abbreviations: M, male; F, female; VCR, vincristine; cyclo, cyclophosphamide; ActD, Dactinomycin; FC, fold-change; SD, stable disease; CR, complete remission

**Table 2. Variant Table**

**Table 2. Variant table**

Patient	Gene 1	Gene 2	Position 1	Position 2	Exon #1	Transcript #1	Exon #2	Transcript #2	Fusion Sequence	HGVS Protein reference	Variant type	Predicted effect	Platform
Patient 1	SPECC1L	NTRK2	chr22:24759948	chr9:87468314	12	NM_015330	15	NM_006180	TCATTGAGAAAATTTTAGCCAGTA AAGTGGGCGGTGGGGGTGGGGGT GGGGGTGGGAGTGGGGGCAGCAG TTTTTAGTAATCAGGGGAAAACA ATTACTGcctggagtctgattctaagaattgct cagctttaaactgtcttc	NM_015330: c.1_2827::N M_006180:c. 1398_* (p.V943::p.D 466)	Breakend	In frame fusion	WGS/RNA
Patient 1	NTRK2	SPECC1L	chr9:87468313	chr22:24759949	14	NM_006180	13	NM_015330	GCCGTTCACTTCTGGCAGTGTCTA GAGAGGGCCACATCTTCTGACA TTCTAGTCCAGCTCTTTATTCCAC ACTACTGacatgtaacatggattgcattaaatcag cccaggaatgatagagttaatggcgcctgcagatccac cttctt				
Patient 1	NTRK2	SPECC1L-ADORA2A	chr9:87468313	chr22:24759949	14	NM_006180	13	ENST00000358654.2	GCCGTTCACTTCTGGCAGTGTCTA GAGAGGGCCACATCTTCTGACA TTCTAGTCCAGCTCTTTATTCCAC ACTACTGacatgtaacatggattgcattaaatcag cccaggaatgatagagttaatggcgcctgcagatccac cttctt				
Patient 1	SPECC1L-ADORA2A	NTRK2	chr22:24759948	chr9:87468314	12	ENST00000358654.2	15	NM_006180	TCATTGAGAAAATTTTAGCCAGTA AAGTGGGCGGTGGGGGTGGGGGT GGGGGTGGGAGTGGGGGCAGCAG TTTTTAGTAATCAGGGGAAAACA ATTACTGcctggagtctgattctaagaattgct cagctttaaactgtcttc				
Patient 2	SPECC1L	NTRK2	chr22:24751499	chr9:87444519	11	NM_015330	15	NM_006180	CCTATCCACCCACCCACCTACCTA CCTACCTACCTATCTAACTATCTT ATTTGTCTGTCTGTCTGCCCTGTCT ATCAAAAACCTGTtccgcctgttgcagctgg gccgttggactctcaccacccggagaggacac agtgagaga	NM_015330: c.1_2743::N M_006180:c. 1398_* (p.E915::p.D4 66)	Breakend	In frame fusion	WGS/RNA
Patient 2	NTRK2	SPECC1L	chr9:87444522	chr22:g.24751501	14	NM_006180	12	NM_015330	CATTGTGCTCTCCAGGCCTTCTCA GGATCTGGTGTGTTGAGTGTCTG TCTGTTGGCCTCTTAAGGGGCGAT GTTCTaagttatactatacctgactccaagccat caccaatgggttcattccagaatttcccttccctactta				
Patient 3	SPECC1L	NTRK3	chr22:24732891	chr15:88646160	9	NM_015330	13	NM_002530	TTTGACTTTACAGTAGTGCCAGCG ATACACATTCAGTACAGCATTACAG TAATTTAAATGAGTTATTCAttatttat aaattattattattataaatgagttattgatgaaggcag ggaccatcaaacgccttcatcaactctgac	NM_015330: c.1_2560::N M_002530:c. 1396_* (p.V854::p.G 466)	Breakend	In frame fusion	WGS/RNA

Abbreviations: WGS, whole genome sequencing; RNA, RNA sequencing. Variants were called based on the GRCh37/hg19 genome build.

## REFERENCES

- Atiq M. A., Davis J. L., Hornick J. L., et al. (2020). Mesenchymal tumors of the gastrointestinal tract with ntrk rearrangements: A clinicopathological, immunophenotypic, and molecular study of eight cases, emphasizing their distinction from gastrointestinal stromal tumor (gist), *Mod Pathol*.
- Bongarzone I., Pierotti M. A., Monzini N., et al. (1989). High frequency of activation of tyrosine kinase oncogenes in human papillary thyroid carcinoma, *Oncogene*, 4: 1457-1462.
- Bourgeois J. M., Knezevich S. R., Mathers J. A., et al. (2000). Molecular detection of the ETV6-NTRK3 gene fusion differentiates congenital fibrosarcoma from other childhood spindle cell tumors, *Am J Surg Pathol*, 24: 937-946.
- Cameron Daniel L., Baber Jonathan, Shale Charles, et al. (2019). Gridss, purple, linx: Unscrambling the tumor genome via integrated analysis of structural variation and copy number, *bioRxiv*: 781013.
- Cancer Genome Atlas Research Network. (2014). Integrated genomic characterization of papillary thyroid carcinoma, *Cell*, 159: 676-690.
- Capper D., Jones D. T. W., Sill M., et al. (2018). DNA methylation-based classification of central nervous system tumours, *Nature*, 555: 469-474.
- Cingolani P., Platts A., Wang le L., et al. (2012). A program for annotating and predicting the effects of single nucleotide polymorphisms, snpeff: SNPs in the genome of drosophila melanogaster strain w1118; iso-2; iso-3, *Fly (Austin)*, 6: 80-92.
- Clarke M., Mackay A., Ismer B., et al. (2020). Infant high grade gliomas comprise multiple subgroups characterized by novel targetable gene fusions and favorable outcomes, *Cancer Discov*.
- Cocco E., Scaltriti M., and Drilon A. (2018). NTRK fusion-positive cancers and TRK inhibitor therapy, *Nat Rev Clin Oncol*, 15: 731-747.
- Davis J. L., Lockwood C. M., Albert C. M., et al. (2018). Infantile NTRK-associated mesenchymal tumors, *Pediatr Dev Pathol*, 21: 68-78.
- Dickson B. C., Swanson D., Charames G. S., et al. (2018). Epithelioid fibrous histiocytoma: Molecular characterization of ALK fusion partners in 23 cases, *Mod Pathol*, 31: 753-762.
- Drilon A., Laetsch T. W., Kummar S., et al. (2018). Efficacy of larotrectinib in TRK fusion-positive cancers in adults and children, *N Engl J Med*, 378: 731-739.
- Fouladi M., Gururangan S., Moghrabi A., et al. (2009). Carboplatin-based primary chemotherapy for infants and young children with CNS tumors, *Cancer*, 115: 3243-3253.
- Gatalica Z., Xiu J., Swensen J., et al. (2019). Molecular characterization of cancers with NTRK gene fusions, *Mod Pathol*, 32: 147-153.
- Gayevskiy V., Roscioli T., Dinger M. E., et al. (2019). Seave: A comprehensive web platform for storing and interrogating human genomic variation, *Bioinformatics*, 35: 122-125.
- Guerreiro Stucklin A. S., Ryall S., Fukuoka K., et al. (2019). Alterations in ALK/ROS1/NTRK/MET drive a group of infantile hemispheric gliomas, *Nat Commun*, 10: 4343.
- Hodgson A., Pun C., Djordjevic B., et al. (2020). NTRK-rearranged cervical sarcoma: Expanding the clinicopathologic spectrum, *Int J Gynecol Pathol*.
- Hsiao Susan J., Zehir Ahmet, Sireci Anthony N., et al. (2019). Detection of tumor ntrk gene fusions to identify patients who may benefit from tyrosine kinase (TRK) inhibitor therapy, *The Journal of Molecular Diagnostics*, 21: 553-571.
- Hung Y. P., Fletcher C. D. M., and Hornick J. L. (2018). Evaluation of pan-TRK immunohistochemistry in infantile fibrosarcoma, lipofibromatosis-like neural tumour and histological mimics, *Histopathology*, 73: 634-644.
- Jennings L. J., Arcila M. E., Corless C., et al. (2017). Guidelines for validation of next-generation sequencing-based oncology panels: A joint consensus recommendation of the association for molecular pathology and college of american pathologists, *J Mol Diagn*, 19: 341-365.
- Knezevich S. R., McFadden D. E., Tao W., et al. (1998). A novel ETV6-NTRK3 gene fusion in congenital fibrosarcoma, *Nat Genet*, 18: 184-187.

- Laetsch T. W., DuBois S. G., Mascarenhas L., et al. (2018). Larotrectinib for paediatric solid tumours harbouring NTRK gene fusions: Phase 1 results from a multicentre, open-label, phase 1/2 study, *Lancet Oncol*, 19: 705-714.
- Li H., and Durbin R. (2009). Fast and accurate short read alignment with burrows-wheeler transform, *Bioinformatics*, 25: 1754-1760.
- Mackay A., Burford A., Carvalho D., et al. (2017). Integrated molecular meta-analysis of 1,000 pediatric high-grade and diffuse intrinsic pontine glioma, *Cancer Cell*, 32: 520-537 e525.
- Marchio C., Scaltriti M., Ladanyi M., et al. (2019). ESMO recommendations on the standard methods to detect NTRK fusions in daily practice and clinical research, *Ann Oncol*, 30: 1417-1427.
- Martin-Zanca D., Hughes S. H., and Barbacid M. (1986). A human oncogene formed by the fusion of truncated tropomyosin and protein tyrosine kinase sequences, *Nature*, 319: 743-748.
- McLaren William, Gil Laurent, Hunt Sarah E., et al. (2016). The ensembl variant effect predictor, *Genome Biology*, 17: 122.
- McWhirter J. R., Galasso D. L., and Wang J. Y. (1993). A coiled-coil oligomerization domain of BCR is essential for the transforming function of BCR-ABL oncoproteins, *Mol Cell Biol*, 13: 7587-7595.
- Murphy D. A., Ely H. A., Shoemaker R., et al. (2017). Detecting gene rearrangements in patient populations through a 2-step diagnostic test comprised of rapid IHC enrichment followed by sensitive next-generation sequencing, *Appl Immunohistochem Mol Morphol*, 25: 513-523.
- Nelson A. W., Schrock A. B., Pavlick D. C., et al. (2019). Novel SPECC1L-MET fusion detected in circulating tumor DNA in a patient with lung adenocarcinoma following treatment with erlotinib and osimertinib, *J Thorac Oncol*, 14: e27-e29.
- Paila U., Chapman B. A., Kirchner R., et al. (2013). Gemini: Integrative exploration of genetic variation and genome annotations, *PLoS Comput Biol*, 9: e1003153.
- Pavlick D., Schrock A. B., Malicki D., et al. (2017). Identification of NTRK fusions in pediatric mesenchymal tumors, *Pediatr Blood Cancer*, 64.
- Penault-Llorca F., Rudzinski E. R., and Sepulveda A. R. (2019). Testing algorithm for identification of patients with TRK fusion cancer, *J Clin Pathol*, 72: 460-467.
- Pinese Mark, Lacaze Paul, Rath Emma M., et al. (2020). The medical genome reference bank contains whole genome and phenotype data of 2570 healthy elderly, *Nature Communications*, 11: 435.
- Rabban J. T., Devine W. P., Sangoi A. R., et al. (2020). NTRK fusion cervical sarcoma: A report of three cases, emphasising morphological and immunohistochemical distinction from other uterine sarcomas, including adenosarcoma, *Histopathology*.
- Roberts K. G., Li Y., Payne-Turner D., et al. (2014). Targetable kinase-activating lesions in Ph-like acute lymphoblastic leukemia, *N Engl J Med*, 371: 1005-1015.
- Rodrigues G. A., and Park M. (1993). Dimerization mediated through a leucine zipper activates the oncogenic potential of the MET receptor tyrosine kinase, *Mol Cell Biol*, 13: 6711-6722.
- Saadi I., Alkuraya F. S., Gisselbrecht S. S., et al. (2011). Deficiency of the cytoskeletal protein SPECC1L leads to oblique facial clefting, *Am J Hum Genet*, 89: 44-55.
- Sahm F., Schimpf D., Jones D. T., et al. (2016). Next-generation sequencing in routine brain tumor diagnostics enables an integrated diagnosis and identifies actionable targets, *Acta Neuropathol*, 131: 903-910.
- Saunders C. T., Wong W. S., Swamy S., et al. (2012). Strelka: Accurate somatic small-variant calling from sequenced tumor-normal sample pairs, *Bioinformatics*, 28: 1811-1817.
- Seager M., Aisner D. L., and Davies K. D. (2019). Oncogenic gene fusion detection using anchored multiplex polymerase chain reaction followed by next generation sequencing, *J Vis Exp*.
- Shen M. M. (2013). Chromoplexy: A new category of complex rearrangements in the cancer genome, *Cancer Cell*, 23: 567-569.

- Sheng W. Q., Hisaoka M., Okamoto S., et al. (2001). Congenital-infantile fibrosarcoma. A clinicopathologic study of 10 cases and molecular detection of the ETV6-NTRK3 fusion transcripts using paraffin-embedded tissues, *Am J Clin Pathol*, 115: 348-355.
- Stransky N., Cerami E., Schalm S., et al. (2014). The landscape of kinase fusions in cancer, *Nat Commun*, 5: 4846.
- Surrey L. F., Jain P., Zhang B., et al. (2019). Genomic analysis of dysembryoplastic neuroepithelial tumor spectrum reveals a diversity of molecular alterations dysregulating the MAPK and PI3K/MTOR pathways, *J Neuropathol Exp Neurol*, 78: 1100-1111.
- Torre Matthew, Vasudevaraja Varshini, Serrano Jonathan, et al. (2020). Molecular and clinicopathologic features of gliomas harboring NTRK fusions, *Acta Neuropathologica Communications*, 8: 107.
- Van der Auwera G. A., Carneiro M. O., Hartl C., et al. (2013). From fastq data to high confidence variant calls: The genome analysis toolkit best practices pipeline, *Curr Protoc Bioinformatics*, 43: 11.10.11-11.10.33.
- Wong Marie, Mayoh Chelsea, Lau Loretta M. S., et al. (2020). Whole genome, transcriptome and methylome profiling enhances actionable target discovery in high-risk pediatric cancer, *Nature Medicine*.
- Zhou X., Edmonson M. N., Wilkinson M. R., et al. (2016). Exploring genomic alteration in pediatric cancer using ProteinPaint, *Nat Genet*, 48: 4-6.



## Recurrent SPECC1L-NTRK fusions in paediatric sarcoma and brain tumours

Dong-Anh Khuong-Quang, Lauren M Brown, Marie Wong, et al.

*Cold Spring Harb Mol Case Stud* published online November 3, 2020  
Access the most recent version at doi:[10.1101/mcs.a005710](https://doi.org/10.1101/mcs.a005710)

---

### Supplementary Material

<http://molecularcasestudies.cshlp.org/content/suppl/2020/11/12/mcs.a005710.DC1>

Published online November 3, 2020 in advance of the full issue.

### Accepted Manuscript

Peer-reviewed and accepted for publication but not copyedited or typeset; accepted manuscript is likely to differ from the final, published version. Published online November 3, 2020 in advance of the full issue.

### Creative Commons License

This article is distributed under the terms of the <http://creativecommons.org/licenses/by-nc/4.0/>, which permits reuse and redistribution, except for commercial purposes, provided that the original author and source are credited.

### Email Alerting Service

Receive free email alerts when new articles cite this article - sign up in the box at the top right corner of the article or [click here](#).

---